Thermoreflection spectra and electron structure of superconducting alloy $Nb_{3+x}Ge_{1-x}$

A. I. Golovashkin, E. V. Pechen', and A. L. Shelekhov

P. N. Lebedev Physics Institute, Academy of Sciences of the USSR, Moscow

(Submitted 15 July 1985)
Zh. Eksp. Teor. Fiz. **90**, 686–696 (February 1986)

The thermoreflection spectra were determined in the range 0.5–3.1 eV for polycrystalline samples of $Nb_{3+x}Ge_{1-x}$ alloys ($x = 0.12, 0.2, 0.32$) and of Nb_5Ge_3. Some characteristics of the electron structure of the A15 phase were determined for $Nb_{3+x}Ge_{1-x}$ and Nb_5Ge_3 and the coefficients in the temperature dependences of the individual characteristics were found. The thermoreflection spectra in the electron structure characteristics of the A15 phase of $Nb_{3+x}Ge_{1-x}$ depended on the composition. These dependences were attributed to broadening of a sharp singularity in the density of the electron states near the Fermi energy as a result of changes in the composition of the A15 phase near stoichiometry. It was found that the change in the electron structure of the A15 phase of the alloys due to deviation of the composition from stoichiometry could not be explained by a simple increase in the number of defects in a sample. In an ideal Nb_3Ge the temperature of the transition to the superconducting state could be above 25 K.

Much work has been done on the properties of high-temperature superconducting transition-metal alloys with the A15 crystal lattice. A special place among these materials is occupied by Nb_3Ge, for which the highest superconducting transition temperatures T_c have been obtained so far. However, the work on Nb_3Ge has been mainly concerned with the superconducting properties of this compound, with the static characteristics, and methods of preparation. This has been primarily due to difficulties in preparing Nb_3Ge samples because of the instability of the A15 phase of this compound. For these,reasons many properties of the compound, particularly the electron structure and the optical characteristics, have not been investigated sufficiently thoroughly.

High values of T_c of Nb_3Ge and anomalies of its other properties (like the anomalies exhibited by other transition-metal alloys with the A15 lattice) are attributed[1–6] to the presence of a narrow peak in the distribution of the density of the electron states $N(E)$ near the Fermi level E_F. The width of this peak is only a few hundredths of an electron volt.[4,5,7] Changes in the concentrations of defects in the samples (and, consequently, in the mean free path of electrons) cause broadening of the peak and associated changes in the other electron characteristics. Such changes have been observed experimentally both for Nb_3Ge and for other materials.[8–10]

Many properties of Nb-Ge alloys, particularly their superconductivity, depend strongly on the concentrations of the components in the A15 phase. Even a slight change in the composition near stoichiometry is known to alter greatly T_c. There are grounds for assuming that such changes in the composition of the A15 phase of Nb-Ge alloys can have a major influence on the electron structure. For example, a change in the composition should result in broadening (or a shift relative to the Fermi level) of the electron state density near E_F and in corresponding changes in the electron characteristics, as well as in the properties of the alloys governed by these characteristics. Moreover, there should be changes in the temperature dependences of the individual characteristics of the electron structure. It would therefore be of interest to study the influence of the composition of the A15 phase of Nb-Ge alloys on their electron structure.

We obtained information on the electron structure of Nb-Ge alloys by the method of thermomodulation optical spectra which has been used successfully in studies of both simple and transition metals and of alloys based on them.[9–12] The intensity in the thermomodulation spectra is governed by the temperature dependences of the characteristics of the electron structure of the investigated material. Therefore, changes in the temperature dependences of the electron characteristics of the A15 phase of Nb-Ge alloys, caused by changes in their compositions, should be manifested primarily in the nature and intensity of the thermomodulation spectra. We determined thermoreflection spectra of some $Nb_{3+x}Ge_{1-x}$ samples with x ranging from 0.1 to 0.3, and also of a sample of the tetragonal σ phase of Nb_5Ge_3, and we determined the composition dependences of some of the electron structure characteristics.

EXPERIMENTAL METHOD

The investigated samples were polycrystalline films deposited on sapphire substrates by the cathodic sputtering method.[13] This procedure took place in an ultrahigh-vacuum system where the argon pressure was 0.8 Torr. Before the deposition of a film the system was pumped down to 10^{-10} Torr. A composite target was used. The temperature of the substrate during the deposition of films was 680 °C. Samples with different concentrations of the components in the A15 phase were obtained by altering the position of the substrate relative to the center of the target along the composition gradient line. The properties of the samples are listed in Table I, where d is the film thickness, T_c is the temperature in

0038-5646/86/020399-08$04.00

TABLE I. Properties of samples

Sample	d, μ	ρ_c/ρ_0	T_c, K	A_0, %	z, %	a_0, Å
$Nb_{3,12}Ge_{0,88}$ (№ 1)	0,27	2	19.3	85	78	5.145
$Nb_{3,2}Ge_{0,8}$ (№ 2)	0.38	1,6	16,5	100	80	5.16
$Nb_{3,32}Ge_{0,68}$ (№ 3)	0,37	1,25	11,5	100	83	5,17
Nb_5Ge_3 (№ 4)	0,35	2.25	–	0	–	$a'=10.16$ $c'=5.14$

the middle of the superconducting transition, a_0 is the lattice constant of the A15 phase, a' and c' are the lattice parameters of the σ phase, A_0 is the content of the A15 phase in the samples, z is the atomic content of niobium in the A15 phase (the content of niobium in the σ phase was 62.5 at.%), ρ_c/ρ_0 is the ratio of the electrical resistivity at a temperature close to T_c and at room temperature. The composition of the samples was determined by the method of x-ray microprobe analysis. An x-ray structure analysis showed that $Nb_{3+x}Ge_{1-x}$ samples Nos. 2 and 3 consisted of a single phase and contained only the A15 phase. Sample No. 1 contained about 8% of the σ phase. Sample No. 4 consisted practically only of the tetragonal σ phase of Nb_5Ge_3.

The optical thermoreflection spectra $\beta(\omega) = d\ln[R(\omega)]/dT$, where $R(\omega)$ is the reflection coefficient, T is the absolute temperature, and ω is the angular frequency of the incident radiation, were determined in the spectral range 0.5–3.1 eV using appratus described earlier.[14] Modulation of the temperature of a sample during these experiments resulted from the passage of current pulses at a repetition frequency of 23 Hz and it amounted to 2–3 K depending on the sample. The depth of the temperature modulation during an experiment was monitored and measured by a method proposed in Ref. 14. Repeated accumulation of the measured signal (each spectrum was recorded several hundreds of times) in the memory of a multichannel analyzer made it possible to record spectra with an average error of the order of 2×10^{-6} K^{-1}.

RESULTS

The experimental thermoreflection spectra of the investigated $Nb_{3+x}Ge_{1-x}$ and Nb_5Ge_3 samples are shown in Fig. 1. The spectra of $Nb_{3+x}Ge_{1-x}$ samples exhibited several absorption bands in the investigated spectral range and these bands were due to electron interband transitions (A-D). The relative intensities of these bands changed from sample to sample. Moreover, there was some band shift in different samples. The main thermoreflection maximum identified by the letter B was located at $\hbar\omega = 2$–2.4 eV. The intensity of this band decreased monotonically between samples Nos. 1 and 3. The amplitude at the maximum fell by about an order of magnitude between these samples. A similar dependence on the composition was exhibited also by the second (C) of the main bands at $\hbar\omega = 1.4$–1.7 eV. Therefore, the strongest temperature dependence of the reflection coefficient (corresponding to the maximum intensity of the main bands in the β spectrum) was exhibited by a sample of $Nb_{3.12}Ge_{0.88}$ with the highest value of T_c and it decreased on increase in nonstoichiometry. A band denoted by A' was regarded by us as a fine structure.

The spectra of the σ phase of Nb_5Ge_3 (sample No. 4) showed clearly three interband absorption bands with maxima at $\hbar\omega = 1.4$, 1.95, and 2.55 eV. The thermoreflection spectrum of this sample and the positions of the bands differed considerably from the form of the spectra and the positions of the bands exhibited by samples with the A15 structure. The intensity of the β spectrum of sample No. 4 was several times greater than the intensity in the thermoreflection spectra of samples 2 and 3. The absence of the features typical of the σ phase from the spectra of samples Nos. 2 and 3 confirmed the results of the x-ray structure analysis indicating that these samples consisted of just one phase. It should be pointed out that the method proposed in Ref. 10 made it possible to estimate quantitatively the content of the second phase in a sample from the modulation spectrum. This information was obtained for a skin layer which was several hundreds of angstroms thick. The experimentally determined modulation spectra were analyzed on a computer

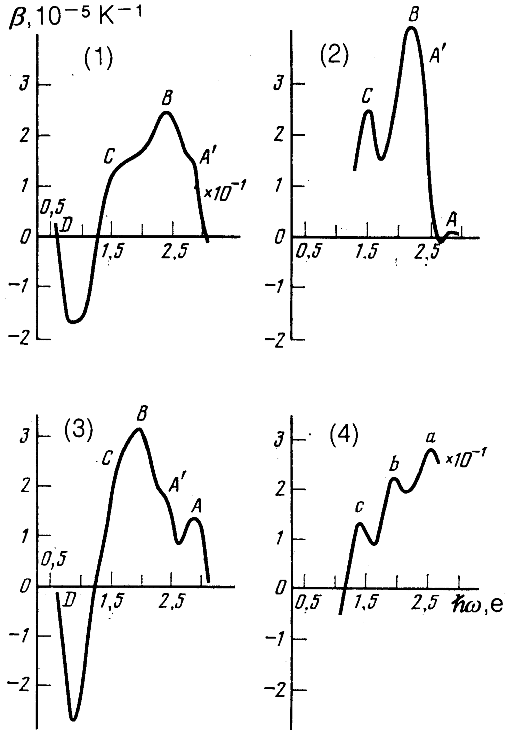

FIG. 1. Experimental thermoreflection spectra of three $Nb_{3+x}Ge_{1-x}$ alloys (1–3) and of Nb_5Ge_3(4). The absorption bands are identified by letters alongside the curves.

using an algorithm and programs developed earlier.[15] It was assumed that the complex permittivity ε' governing the reflection coefficient of light in the investigated part of the spectrum included contributions from intraband (Drude) and interband transitions.

The Drude contribution is governed by the conduction electron density N_e (more correctly, by the ratio N_e/m, where m is the electron mass) and by the effective collision frequency ν_e. The contribution of the interband transitions giving rise to singularities in the thermoreflection spectra in the investigated range of frequencies is governed by the energy gap $E_g = \hbar\omega_g$, relaxation time ν_g^{-1} of electrons participating in the interband transitions, and effective electron density N_g participating in these transitions; the index g refers to different bands A-D and it represents the direction of symmetry in the momentum space (different Bragg planes). In fact, the profile of the ε' band is governed in this model by the resonance factor $[E_g^2 - (\hbar\omega + i\hbar\nu_g)^2]^{-1}$ in the integrand in Eq. (11) of Ref. 16 (i.e., it is governed by the presence of a significant region in the phase space where the energy bands are parallel) and its amplitude is governed by N_g (Ref. 9).

The experimental thermoreflection spectra were approximated by the method of least squares using theoretical curves plotted on the basis of this model. Since, in principle, the β spectra of Nb_3Ge should be affected by the σ phase, we used the model of thermomodulation spectra of a two-phase sample[10] in which an allowance is made for the influence of the second phase on the resultant spectrum. The electron characteristics of the σ phase were the data obtained from the thermoreflection spectra of sample No. 4. The thermoreflection spectra were approximated by varying the characteristics of the conduction electrons (N_e and ν_e), the characteristics of the interband absorption bands (E_g, ν_g, and N_g), the coefficients K_E of the temperature dependences of the energy gaps (values of E_g), the corresponding coefficients K_ν of the collision frequencies (values of ν_e and ν_g), the coefficients K_N of the conduction electron density; the concentration of the A15 phase in a sample (A_0) was also used for this purpose.

The characteristics of the electron structure obtained as a result of an analysis of the experimental thermoreflection spectra are given in Tables II and III. The spectral bands (and the corresponding characteristics in the form of the energy gap E_g, relaxation time ν_g^{-1}, and effective density N_g of electrons participating in interband transitions) of the σ phase are denoted by the indices 1–3. The rest of the notation for the σ phase is the same as that for the A15 phase.

The errors in the determination of the electron characteristics representing interband electron transitions did not exceed 2%, with the exception of N_g, for which the error was 10–20%. The densities and collision frequencies of the conduction electrons were found to within 4–7%. The error in the determination of the temperature dependence coefficients K_E, K_ν, and K_N was 40–50%, whereas the error in the concentration A_0 was 2–4%.

Table II lists also the mean free path of electrons l, the average Fermi velocity v_F, and the density of the electron states near the Fermi energy $N(E_F)$. The values of the electron state density $N(E_F)$ were determined at $T \approx 300$ K by linear interpolation of the values of $N(E_F)$ found experimentally for Nb_3Ge (Ref. 17) and Nb_4Ge (Ref. 18). A correction was made for the temperature dependence of $N(E_F)$ (Ref. 8). The values of $N(E_F)$ given in Table II corresponded to the niobium concentrations in the A15 phase found in the investigated samples. The values of the average Fermi velocity at $T \approx 300$ K were deduced from $N_e/m = (2/3)N(E_F)v_F^2$.

It is clear from Table II that the concentration of the A15 phase in the samples agreed well with the results of an x-ray structure analysis given in Table I.

Ellipsometric measurements were used in Ref. 19 to obtain some of the parameters of the electron structure of Nb–Ge alloys. A comparison of the characteristics (T_c, ρ_c/

TABLE II. Electron characteristics of A15 phase of $Nb_{3.32}Ge_{0.68}$ samples

Characteristic	$Nb_{3,12}Ge_{0,88}$ (№ 1)	$Nb_{3,2}Ge_{0,8}$ (№ 2)	$Nb_{3,32}Ge_{0,68}$ (№ 3)
N_e, 10^{22} cm^{-3}	0.85	1,2	1.4
ν_e, 10^{14} sec^{-1}	2,7	1.7	1.5
E_A, eV	3.36	2.88	2.84
E_B, eV	1,96	2.04	1.48
E_C, eV	1,22	1,26	0,96
E_D, eV	0.56	0,60	0,52
ν_A, 10^{14} sec^{-1}	1.0	4,7	4.4
ν_B, 10^{14} sec^{-1}	17	6.4	13
ν_C, 10^{14} sec^{-1}	5.9	7.2	8.4
ν_D, 10^{14} sec^{-1}	0.6	2.9	2.7
N_A, 10^{22} cm^{-3}	0,02	0.01	0.01
N_B, 10^{22} cm^{-3}	0.13	0.04	0.1
N_C, 10^{22} cm^{-3}	0.1	0,11	0.08
N_D, 10^{22} cm^{-3}	0.14	0,2	0,2
K_N, 10^{-4} K^{-1}	3.3	6	6
K_E, 10^{-4} K^{-1}	−8	−0.2	−0.1
K_ν, 10^{-3} K^{-1}	3	2	2
A_0, %	91	100	98
v_F, 10^8 cm/sec	0.3	0.37	0.4
$N(E_F)$, states·(eV·at·spin)$^{-1}$	0,42	0.40	0.37
l, Å	11	22	26

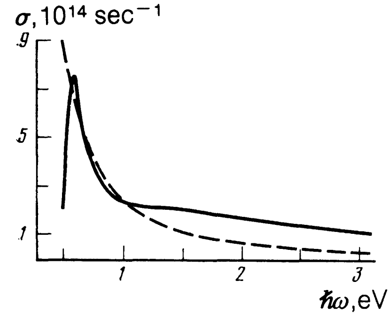

FIG. 2. Spectral depedences of the contributions made to the optical conductivity of $Nb_{3.12}Ge_{0.88}$ by the conduction electrons (dashed curve) and by the electrons participating in the interband transitions (continuous curve).

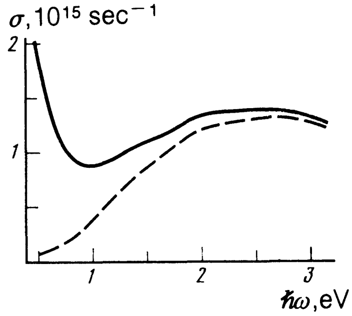

FIG. 3. Optical conductivity spectra $\sigma(\omega)$ of the σ phase of Nb_5Ge_3 and the contributions made to this conductivity by the interband transitions (dashed curve), deduced on the basis of the data in Table III.

ρ_0, a_0) of the investigated samples showed that the alloys used in Ref. 19 had similar parameters to those of our samples Nos. 2 and 3. The electron characteristics of sample No. 3 obtained from the thermoreflection spectra were not in conflict with the results of Ref. 19. The parameters of the individual bands in these spectra agreed well and the densities N_e were practically identical.

The plasma oscillation frequency ω_{pl} (in energy units) calculated from the values of N_e in Table II was 3.4, 4.0, and 4.4 eV for samples Nos. 1, 2, and 3. The composition of sample No. 1 was closest to Nb_3Ge. A comparison of $\hbar\omega_{pl}$ for the first sample with the published data on Nb_3Ge indicated that it was somewhat less than 3.7 eV calculated theoretically in Refs. 3 and 20, and slightly more than $\hbar\omega_{pl} = 3.2$ eV found experimentally at $T = 230$ K by Yao and Schnatterly and quoted in Ref. 21. Bearing in mind that the composition of the samples used by Yao and Schnatterly was quite close to stoichiometric, we found that the value of ω_{pl} of the A15 phase decreased smoothly on increase in the atomic concentration of Ge.

The electron characteristics of the A15 phase of different compositions and of the σ phase of Nb-Ge alloys obtained from the thermoreflection spectra allowed us to calculate the dispersion dependences of the real and imaginary parts of the permittivity of these phases, and also of the other optical characteristics. Figure 2 shows the spectral (dispersion) dependences of the contributions to the optical conductivity of $Nb_{3.12}Ge_{0.88}$ governed by the conduction electrons (dashed curve) and by the electrons participating in the interband transitions (continuous curve). In the investigated part of the spectrum the conduction electrons made a considerable contribution to the permittivity and this allowed us to determine the characteristics of these electrons with a satisfactory precision.

Figure 3 shows the optical conductivity spectrum $\sigma(\omega)$ and the contributions made to this spectrum by the interband transitions $\sigma_b(\omega)$ in the σ phase of Nb_5Ge_3. The spectrum was calculated on the basis of the data in Table III which were deduced from the experimental thermoreflection spectrum of sample No. 4. It should be pointed out that the difference between the optical characteristics of the alloys due to changes in the composition of the A15 phase were manifested particularly clearly in the β spectra of the investigated samples. In the $\sigma(\omega)$ curves the sharpness of the individual absorption bands was concealed by a significant contribution of the Drude component.

Figure 4 shows the contributions made to the thermoreflection spectrum of the A15 phase of sample No. 1 by the temperature dependences of the real ε_1 and imaginary ε_2 parts of the permittivity in accordance with the expansion

$$\beta(\omega) = \Delta R/R\Delta T = [a(\varepsilon_1; \varepsilon_2)\Delta\varepsilon_1 + b(\varepsilon_1; \varepsilon_2)\Delta\varepsilon_2]/\Delta T.$$

The quantities $\Delta\varepsilon_1$ and $\Delta\varepsilon_2$ represent here the changes in ε_1 and ε_2 due to a small change in temperature ΔT. The coefficients $a(\varepsilon_1;\varepsilon_2)$ and $b(\varepsilon_1;\varepsilon_2)$ in the above expression were calculated using the formulas in Ref. 10. It was shown in Ref. 9 that in the region of the main interband absorption bands the thermoreflection spectrum of niobium is governed largely by the contribution of the temperature change in ε_1. This was also demonstrated for aluminum. On the other hand, the thermomodulation spectra of Nb_3Sn and Nb_3Al

TABLE III. Electron characteristics of σ phase of Nb_5Ge_3

Characteristic		Characteristic	
N_e, 10^{22} cm^{-3}	2.6	N_1, 10^{22} cm^{-3}	1.52
ν_e, 10^{14} sec^{-1}	1.8	N_2, 10^{22} cm^{-3}	0.46
E_1, eV	2.54	N_3, 10^{22} cm^{-3}	0.78
E_2, eV	1,88	K_E, 10^{-4} K^{-1}	−2,6
E_3, eV	1.22	K_ν, 10^{-3} K^{-1}	3
ν_1, 10^{15} sec^{-1}	1.18	A_0, %	0
ν_2, 10^{15} sec^{-1}	0.56	K_N, 10^{-4} K^{-1}	0
ν_3, 10^{15} sec^{-1}	0,8		

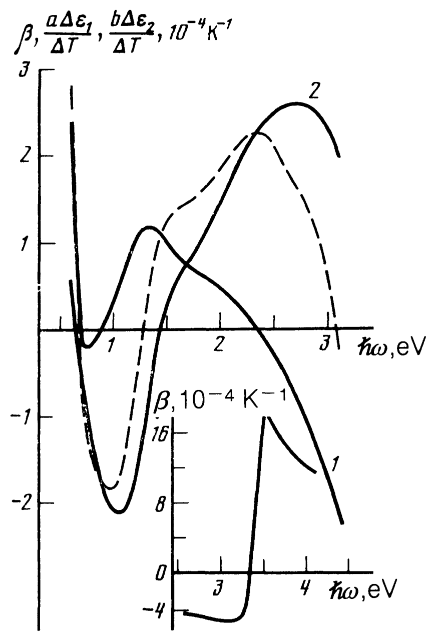

FIG. 4. Contributions to the thermoreflection spectra of the A15 phase of sample No. 1 (dashed curve) made by the temperature dependences of the real ε_1 (curve 1) and imaginary ε_2 (curve 2) parts of the permittivity. The inset shows the β spectrum of sample No. 1 calculated in the plasma frequency region allowing only for the contribution of the conduction electrons.

alloys were found to be dominated by the temperature dependence of ε_2 (Ref. 10). It is clear from Fig. 4 that the structure of the β spectrum of Nb_3Ge is also governed mainly by the contribution of $\Delta\varepsilon_2(\omega)$. However, in the region of 1.5 and 3 eV the β spectrum includes also a large contribution from $\Delta\varepsilon_1$. Therefore, depending on the characteristics of the electron structure of a specific metal or alloy, its thermomodulation optical spectrum may be governed by the temperature dependences of ε_1 or ε_2. The inset in Fig. 4 shows the thermoreflection spectrum of sample No. 1 in the plasma frequency range calculated allowing only for the contribution of the conduction electrons.

DISCUSSION

1. The data given in Table II demonstrate a definite dependence of the electron characteristics of the A15 phase of $Nb_{3+x}Ge_{1-x}$ alloys on the composition. Since a reduction in the amount of niobium in the A15 phase reduces the conduction electron density, the collision frequency ν_e rises. There is also a definite composition dependence in the case of the characteristics representing the interband transitions. The minimum values of the energy gaps are obtained for sample No. 3 with the A15 phase characterized by the largest amount (83%) of niobium. Figure 5 shows the dependences of N_e, ν_e, $N(E_F)$, v_F, a_0, and T_c on the composition of the A15 phase of the investigated samples. It should be pointed out that the curves in Fig. 5 are purely qualitative.

The observed composition dependences of the electron characteristics can be explained on the hypothesis that an increase in the niobium concentration in the A15 phase, i.e., the progression from sample No. 1 to samples Nos. 2 and 3, results in the replacement of germanium with niobium atoms. Theoretical calculations[3] show that the replacement of transition metal atoms with nontransition metal atoms in the A15 structure broadens the sharp singularities in the density of the electron states $N(E)$. Moreover, such a replacement, accompanied by a departure from the ideal germanium sublattice, is equivalent to some disordering of the structure, i.e., it gives rise to structure defects. This in turn should result in additional broadening of the sharp singularities of $N(E)$. The broadening of a peak of the electron state density is proportional to the defect concentration.[22] Therefore, if the energy position of such a peak is close to E_F, a change in the composition (increase in the concentration of Nb) should reduce the density of the electron states on the $N(E_F)$ surface and alter other electron characteristics: it should reduce T_c, increase the density of the conduction electrons and also the average velocity of electrons on the Fermi surface. This should also be near the energy gaps and reduce the maxima in the temperature dependences of the electron characteristics. This is exactly the behavior exhibited by $Nb_{3+x}Ge_{1-x}$ samples. A change in the composition can naturally result also in more complex changes in the electron structure, for example, it may shift the peak of $N(E)$ relative to E_F.

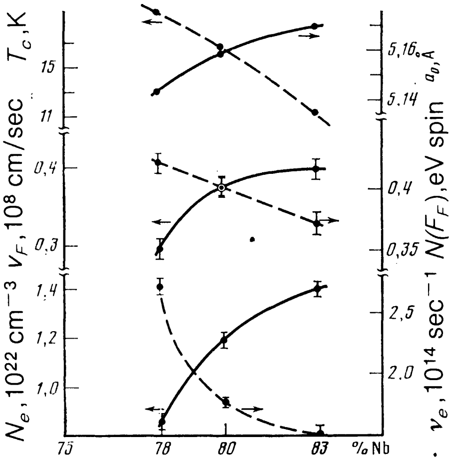

FIG. 5. Dependences of some characteristics of the electron structure of the A15 phase of Nb-Ge alloys, and the dependences of T_c and a_0 on the composition.

For a given composition of the phase the broadening of a peak of $N(E)$ is favored by several factors, such as the rise of temperature or the presence of impurities, stresses, and other defects in the lattice. These factors affect the electron characteristics of the samples. The maximum changes in the parameters associated with the broadening of the peak of the density of electron states should be observed for $\delta E/\hbar\nu_e < 1$, where δE is the energy width of the peak. In the case of samples of different compositions the relative influence of these factors may be different. We should also bear in mind an increase in the strength of the electron-phonon interaction in the high-temperature phase which—other conditions being equal—reduces the mean free path l of electrons and increases the effective frequency ν_e of electron collisions. An allowance not only for a change in the compositon of the A15 phase, but also for other defects (such as those represented by the value of l) can account for the observed behavior of the electron characteristics of the investigated films.

The results show that the effect of the composition is even greater on the density of the conduction electrons (effective mass).

2. The observed changes in the intensities in the thermoreflection spectra of $Nb_{3+x}Ge_{1-x}$ due to changes in the compositon of the A15 phase confirm the hypothesis that the composition influences the electron structure; it can also be explained assuming a sharp singularity in the distribution of the density of electron states near the Fermi energy. The strongest temperature dependence of the electron characteristics exhibited by sample No. 1 corresponds to the maximum intensity in the thermoreflection spectrum. The results obtained for $Nb_{3+x}Ge_{1-x}$ alloys indicate that changes in the composition of the A15 phase have an effect on the electron structure which is more complex than a simple change in the number of defects.

3. Extrapolation of the composition dependences of the electron characteristics of $Nb_{3+x}Ge_{1-x}$ alloys to the stoichiometric composition (i.e., to $x = 0$) can give the characteristics of an "ideal" compound Nb_3Ge so that in principle its optical and other properties can be calculated. In the first approximation, such extrapolation shows that in the case of ideal Nb_3Ge we can expect $T_c \gtrsim 25$ K, $a_0 \lesssim 5.13$ Å, and also at room temperature we can expect $N_e \lesssim 0.6 \times 10^{22}$ cm^{-3} and $N(E_F) \gtrsim 0.45$ states (eV^{-1}·at·spin)$^{-1}$.

Figure 6 shows the dependences of the critical superconducting transition temperature T_c (measured in the middle of the transition) on the density of the electron states $N(E_F)$. Variation of $N(E_F)$ is due to variation of the composition of the A15 phase of the alloys. It is clear from the figure that the dependence is nearly linear. Extrapolation of this dependence shows that we can expect $T_c \gtrsim 25$ K for the stoichiometric composition using the value of $N(E_F)$ for ideal Nb_3Ge found in Ref. 17. This is in agreement with the maximum value of T_c which has been obtained so far for Nb_3Ge (Refs. 23 and 24).

4. In our analysis of the experimental β spectra we used a theoretical model relating the absorption bands to the presence of parallel parts of the energy bands in the momentum space. If such parallel parts of the energy bands are regarded as the Bragg splitting of the energy levels, the energy gaps E_g can be used to determine the Fourier components of the pseudopotential $V_g = E_g/2$. In this interpretation an identification of the A-D bands in the β spectra of $Nb_{3+x}Ge_{1-x}$, carried out in accordance with the method of Ref. 15, yields $V_{200} = 1.68$, $V_{210} = 0.88$, $V_{211} = 0.61$, and $V_{220} = 0.28$ eV for the first sample (the corresponding values can be obtained similarly for the other samples). It follows that the band A appears because of the influence of the {200} Bragg planes, whereas the bands B, C, and D are due to the {210}, {211}, and {220} planes.

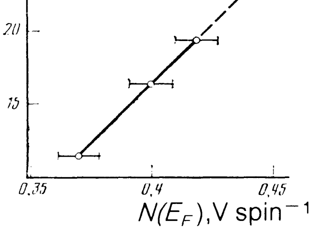

FIG. 6. Dependence of the temperature of the transition to the superconducting state T_c of $Nb_{3+x}Ge_{1-x}$ alloys on the density of electron states $N(E_F)$. An asterisk is used for the value of T_c corresponding to $N(E_F) = 0.45$ states·(eV·at·spin)$^{-1}$ obtained in Ref. 17.

This interpretation is not unique. The observed absorption bands may be attributed also to electron transitions from the d energy band to the Fermi level and from states close to the Fermi level to vacant d energy bands. The main contribution to the absorption is in this case due to regions with quasiparallel energy bands. The profile of each absorption band then changes only slightly.[25] More complex approaches are also possible. In such cases the temperature dependences of the β spectra are extemely important for the determination of the true nature of the absorption bands.

The adopted interpretation in the case of Nb (Ref. 9) and Nb_3Sn (Ref. 10) ensurs agreement between the electron characteristics and the optical spectra, deduced from the thermomodulation spectra, with the results obtained by other methods.

5. It is clear from Table II that in the case of $Nb_{3+x}Ge_{1-x}$ alloys the effective electron collision frequency obeys $\nu_e \propto N_e^{-1}$. It is interesting to note that the data[10] for Nb_3Sn and the best sample of Nb_3Al fit the same dependence. We can account for this result by assuming that, as the composition of the A15 phase moves away from stoichiometry, there is a reduction in the relative change in the density of states $N(E_F)$ associated with the broadening of the $N(E)$ peak by an amount $\hbar\nu_e$. It should be pointed out that broadening of the $N(E)$ peak is due to collisions of electrons both with defects[22,26] and with phonons, i.e., $\nu_e = \nu_{ep} + \nu_{ed}$, where ν_{ep} and ν_{ed} are, respectively, the frequencies of collisions of electrons with phonons and defects. The quantity $\hbar\nu_{ed}$ is proportional to the concentration of defects.

Table II shows also that there is a correlation between T_c and N_e (T_c falls on increase in N_e), observed earlier for other alloys with the A15 lattice. We can also see that T_c rises on increase in ν_e. The data in Tables I and II allow us to estimate readily [ignoring the temperature dependence of N_e compared with $\nu_e(T)$] the frequencies of electron—phonon collisions in samples 1, 2, and 3 which correspond to the energies $\hbar\nu_{ep}$ amounting to 9×10^{-2}, 4×10^{-2}, and 2×10^{-2} eV, respectively. Therefore, the dependence of T_c on ν_e is due to the dependence of T_c on ν_{ep}, i.e., on the electron-phonon interaction constant $\lambda \propto \nu_{ep}$ (Ref. 27).

6. In the range $T \lesssim 50$ K the temperature dependence of the electrical resistivity ρ of the A15 compounds is quadratic:

$$\rho = \rho_0 + \alpha T^2, \qquad (1)$$

where ρ_0 is the residual resistivity. In the case of our

$Nb_{3+x}Ge_{1-x}$ samples the temperature dependence $\rho(T)$ found in this range can also be described quite accurately by the quadratic law (1). Such a quadratic dependence is frequently attributed to the contribution of electron-electron collisions.[28,29] According to Gurzhi,[30] the optical-frequency contribution of the electron-electron collisions $\nu_{ee}^{\rm opt}$ to the effective collision frequency ν_e of the conduction electrons is as follows:

$$\nu_{ee}{}^{\rm opt} = \nu_{ee}[1+(\hbar\omega/2\pi kT)^2]. \tag{2}$$

Here, $\nu_{ee} \propto T^2$ is the classical frequency of electron-electron collisions which governs the term in ρ quadratic in respect of T. We can show that

$$\nu_{ee} = (\alpha/\gamma\rho_0)T^2\nu_e, \tag{3}$$

$$\nu_{ee}{}^{\rm opt} = (\hbar\omega/2\pi kT)^2(\alpha/\gamma\rho_0)\nu_e. \tag{4}$$

Here, $\gamma = \rho/\rho_0$. Equation (4) is derived on the assumption that: 1) the contribution of the electron-electron collisions is retained up to a temperature T (at which the measurements of ν_e are made); 2) $\hbar\omega \gg 2\pi kT$; 3) the electron characteristics N_e and v_F do not vary strongly with T.

The effective collision frequency ν_e measured experimentally contains contributions due to the collisions of electrons with phonons, impurities, and defects, and also with other electrons. In our case the value of ν_e was found from optical measurements at room temperature. In the case of samples of sufficiently high quality with $T_c = 18$–22 K it was found that $\gamma_c = \rho_c/\rho_0 = 1.6$–$2.2$, $\alpha = (2.1$–$4.4)\times 10^{-3}\mu\Omega\cdot{\rm cm}\cdot K^{-2}$, $\alpha/\rho_0 = 3\times 10^{-5} - 1\times 10^{-4}$ K^{-2}. We can then estimate from Eq. (3) that at temperatures close to the room value we have $\nu_{ee} \approx (2$–$5)\times 10^{-5}T^2\nu_e$ (here, T is in degrees Kelvin). Therefore, at $T = T_{\rm room}$ the value of ν_{ee} should exceed the total collison frequency. Moreover, the value of $\nu_{ee}^{\rm opt}$ in the investigated part of the spectrum ($\hbar\omega = 1$–3 eV) should be two orders of magnitude higher than the measured value of ν_e.

An analysis of this contradiction leads to the following conclusions. Some reduction in the approximate value of ν_{ee} at room temperature may result from an allowance for the temperatue dependences of the electron characteristics N_e and v_F (Ref. 8). Broadening of the peak of the density of electron states near E_F on increase in T has the effect that the value of ν_{ee}/T^2 at $T_{\rm room}$ is considerably less than at low temperatures. However, the main reason is that the quadratic dependence $\rho(T)$ observed for Nb_3Ge at low temperatures is not due to electron-electron collisions. It may be explained by the electron-phonon scattering[31] or by the influence of the thermal broadening of the peak of the density of electron states.[22]

A similar conclusion can be drawn for other A15 compounds such as Nb_3Sn and Nb_3Al, for which the temperature dependence $\rho(T)$ is known at low temperatures and the coefficient α is given in Ref. 31, whereas ν_e is given in Ref. 10.

7. In spite of conclusion that the influence of electron-electron collisions on $\rho(T)$ is small, it should be possible to detect the contribution of these collisions in the optical range because of the large factor $(\hbar\omega/2\pi kT)^2$ in $\nu_{ee}^{\rm opt}$. In particular, the influence of electron-electron collisions on the optical properties may be manifested by a contribution to the collision frequency ν_g of electrons participating in the interband transitions. If the anisotropy of ν_g is weak, then in the case of a significant contribution of electron-electron collisions to the relaxation process, we have $\nu_g = \nu_{g0} + \alpha_0 E_g^2$. Here, α_0 is a constant, whereas ν_{g0} is governed by the contribution of other (apart from electron–electron) relaxation processes. This dependence of ν_g on E_g is due to the fact that the energy gap E_g is proportional to the effective frequency ω_g at which ν_g is determined.

The published experimental results show that a quadratic dependence of ν_g on E_g is obeyed quite well in the case of Nb_3Al (Ref. 10). In the case of $Nb_{3+x}Ge_{1-x}$ the characteristics of a band (A) observed in the high-frequency parts of the thermoreflection spectra do not fit this dependence. This may be due to, for example, proximity of the plasma oscillation frequency.

[1] L. F. Mattheiss, Phys. Rev. B **12**, 2161 (1975).

[2] L. F. Mattheiss, L. R. Testardi, and W. W. Yao, Phys. Rev. B **17**, 4640 (1978).

[3] W. E. Pickett, K. M. Ho, and M. L. Cohen, Phys. Rev. B **19**, 1734 (1979).

[4] K. M. Ho, M. L. Cohen, and W. E. Pickett, Phys. Rev. Lett. **41**, 815 (1978).

[5] A. S. Aleksandrov and V. F. Elesin, Fiz. Tverd. Tela (Leningrad) **25**, 456 (1983) [Sov. Phys. Solid State **25**, 257 (1983)].

[6] L. P. Gor'kov, Piz'ma Zh. Eksp. Teor. Fiz. **20**, 571 (1974) [JETP Lett. **20**, 260 (1974)]; Prog. Low Temp. Phys. **7B**, 517 (1978).

[7] A. I. Golovashkin, I. S. Levchenko, G. P. Motulevich, E. V. Pechen', and A. L. Shelekhov, Fiz. Tverd. Tela (Leningrad) **26**, 69 (1984) [Sov. Phys. Solid State **26**, 39 (1984)].

[8] A. I. Golovashkin, E. V. Pechen', and N. P. Shabanova, Zh. Eksp. Teor. Fiz. **82**, 850 (1982) [Sov. Phys. JETP **55**, 503 (1982)]; Materialy 2-go nauchnogo seminara "Metallofizika sverkhprovodnikov" (Proc. Second Scientific Seminar on "Metal Physics of Superconductors"), Kiev, 1983, p. 92.

[9] A. I. Golovashkin and A. L. Shelekhov, Zh. Eksp. Teor. Fiz. **84**, 2141 (1983) [Sov. Phys. JETP **57**, 1246 (1983)].

[10] A. I. Golovashkin, I. S. Levchenko, and A. L. Shelekhov, Zh. Eksp. Teor. Fiz. **86**, 2229 (1984) [Sov. Phys. JETP **59**, 1298 (1984)].

[11] J. H. Weaver, D. W. Lynch, C. H. Culp, ad R. Rosei, Phys. Rev. B **14**, 459 (1976).

[12] G. A. Frazier and R. Glosser, Solid State Commun. **41**, 245 (1982).

[13] A. I. Golovashkin and E. V. Pechen', Fiz. Nizk. Temp. **6**, 454 (1980) [Sov. J. Low Temp. Phys. **6**, 215 (1980)].

[14] A. I. Golovashkin and A. L. Shelekhov, Prib. Tekh. Eksp. No. 5, 216 (1980); Preprint No. 71 [in Russian], Lebedev Physics Institute, Academy of Sciences of the USSR, M., 1979.

[15] A. I. Golovashkin and A. L. Shelekhov, Kratk. Soobshch. Fiz. No. 5, 11 (1978); Preprints Nos. 96 and 134 [in Russian], Lebedev Physics Institute, Academy of Sciences of the USSR, M., 1981.

[16] A. I. Golovashkin and G. P. Motulevich, Zh. Eksp. Teor. Fiz. **57**, 1054 (1969) [Sov. Phys. JETP **30**, 575 (1970)].

[17] G. R. Stewart, L. R. Newkirk, and F. A. Valencia, Solid State Commun. **26**, 417 (1978).

[18] G. R. Stewart, L. R. Newkirk, and F. A. Valencia, Phys. Rev. B **20**, 3647 (1979).

[19] N. D. Kuz'michev, I. S. Levchenko, and G. P. Motulevich, Fiz. Met. Metalloved. **56**, 266 (1983).

[20] P. B. Allen, W. E. Pickett, K. M. Ho, and M. L. Cohen, Phys. Rev. Lett. **40**, 1532 (1978).

[21] I. Tütto, L. M. Kahn, and J. Ruvalds, Phys. Rev. B **20**, 952 (1979).

[22] V. F. Elesin and A. S. Aleksandrov, Vopr. At. Nauki Tekh. Ser. Fiz. Radiats. Povrezhd. Radiats. Materialoved. No. 3(31), 3(1984).

[23] A. I. Golovashkin, E. V. Pechen', A. I. Skvortsov, and N. E. Khlebova, Fiz. Tverd. Tela (Leningrad) **23**, 1324 (1981) [Sov. Phys. Solid State **23**, 774 (1981)].

[24] A. I. Golovashkin and E. V. Pechen', Tr. Fiz. Inst. Akad. Nauk SSSR **151**, 63 (1984).

[25] A. I. Golovashkin and T. I. Kuznetsova, Kratk. Soobshch. Fiz. No. 2, 22 (1984).

[26] A. S. Aleksandrov, V. F. Elesin, M. A. Kotov, V. V. Ogurtsov, A. E. Parshakov, and A. A. Filippov, Zh. Eksp. Teor. Fiz. **87**, 1432 (1984) [Sov. Phys. JETP **60**, 823 (1984)].

[27] J. J. Hopfield, Comments Solid State Phys. **3**, 48 (1970).

[28] D. L. Mills and P. Lederer, J. Phys. Chem. Solids **27**, 1805 (1966).

[29] V. A. Marchenko, Fiz. Tverd. Tela (Leningrad) **15**, 1893 (1973) [Sov. Phys. Solid State **15**, 1261 (1973)].

[30] R. N. Gurzhi, Zh. Eksp. Teor. Fiz. **35**, 965 (1958) [Sov. Phys. JETP **8**, 673 (1959)].

[31] G. W. Webb, Z. Fisk, J. J. Engelhardt, and S. D. Bader, Phys. Rev. B **15**, 2624 (1977).

Translated by A. Tybulewicz